



**CENTRE DE RECERCA MATEMÀTICA**

This is a preprint of: *Evolutionary escape on complex genotype-phenotype networks*

Journal Information: *Journal of Theoretical Biology*,

Author(s): E. Ibanez-Marcelo, T. Alarcon.

Volume, pages: 394 1-14, DOI:[[doi.org/10.1016/j.jtbi.2015.12.033](https://doi.org/10.1016/j.jtbi.2015.12.033)]



# Evolutionary escape on complex genotype–phenotype networks

Esther Ibáñez-Marcelo <sup>a,b,\*</sup>, Tomás Alarcón <sup>e,a,c,d</sup>



<sup>a</sup> Centre de Recerca Matemàtica, Edifici C, Campus de Bellaterra, 08193 Bellaterra (Barcelona), Spain

<sup>b</sup> Departament de Matemàtica Aplicada I, Universitat Politècnica de Catalunya, 08028 (Barcelona), Spain

<sup>c</sup> Departament de Matemàtiques, Universitat Autònoma de Barcelona, 08193 Bellaterra (Barcelona), Spain

<sup>d</sup> Barcelona Graduate School of Mathematics (BGSMath), (Barcelona), Spain

<sup>e</sup> ICREA (Institució Catalana de Recerca i Estudis Avançats), Spain

## HIGHLIGHTS

- We perform a comparative analysis between escape on regular hypercube (*H*-graphs) and complex genotype–phenotype spaces (*B*-graphs).
- We find that the distribution of distances between phenotypes in *B*-graphs exhibits a much larger degree of heterogeneity than in *H*-graphs.
- This property causes heterogeneous behaviour in all results associated to the escape problem.
- Our main result is that the escape probability can be underestimated by assuming a regular hypercube genotype network.

## ARTICLE INFO

### Article history:

Received 25 March 2015

Received in revised form

22 December 2015

Accepted 25 December 2015

Available online 21 January 2016

### Keywords:

Escape

Genotype–phenotype map

Resistance

## ABSTRACT

We study the problem of evolutionary escape that is the process whereby a population under sudden changes in the selective pressures acting upon it try to evade extinction by evolving from previously well-adapted phenotypes to those that are favoured by the new selective pressure. We perform a comparative analysis between results obtained by modelling genotype space as a regular hypercube (*H*-graphs), which is the scenario considered in previous work on the subject, to those corresponding to a complex genotype–phenotype network (*B*-graphs). In order to analyse the properties of the escape process on both these graphs, we apply a general theory based on multi-type branching processes to compute the evolutionary dynamics and probability of escape. We show that the distribution of distances between phenotypes in *B*-graphs exhibits a much larger degree of heterogeneity than in *H*-graphs. This property, one of the main structural differences between both types of graphs, causes heterogeneous behaviour in all results associated to the escape problem. We further show that, due to the heterogeneity characterising escape on *B*-graphs, escape probability can be underestimated by assuming a regular hypercube genotype network, even if we compare phenotypes at the same distance in *H*-graphs. Similarly, it appears that the complex structure of *B*-graphs slows down the rate of escape.

© 2016 Elsevier Ltd. All rights reserved.

## 1. Introduction

Evolutionary escape is the process whereby a population under sudden changes in the selective pressures acting upon it try to evade extinction by evolving from previously well-adapted phenotypes to those that are favoured by the new selective pressure. This evolutionary process is driven by gene mutations. Examples of biological situations where this process is relevant include viruses evading anti-microbial therapy, emergence of drug resistance in

cancer, parasites trying to infect a new host, or species attempting to invade a new ecological niche (Iwasa et al., 2003).

Previous models of evolutionary escape have been developed by Iwasa et al. (2003), Iwasa et al. (2004). They base their approach on the assumption that *n* point mutations in some crucial parts of the genome are necessary for escape. They further assume that the different mutants can be described by binary strings (with entries of +1 or −1) of length *n*. There are  $2^n - 1$  such mutants. It is assumed that the new selective pressures, such as those associated to the administration of a drug, reduce the proliferation ratios, *R*, of sensitive genotypic variants,  $R < 1$ ; whereas resistant genotypes are such that  $R > 1$ . The corresponding evolutionary dynamics is modelled in terms of Galton–Watson multi-type branching process (GWMBP) (Kimmel and Axelrod, 2002), where at each generation each individual of each type has a given (in general, genotype-dependent) probability of mutating and

\* Corresponding author at: Centre de Recerca Matemàtica, Edifici C, Campus de Bellaterra, 08193 Bellaterra (Barcelona), Spain. Tel.: +34 93 581 1081.

E-mail address: [eibanez@crm.cat](mailto:eibanez@crm.cat) (E. Ibáñez-Marcelo).

producing offspring belonging to a different type. The problem is to calculate the probability that an escape genotype is reached starting from a single individual of non-resistant genotype. The model proposed by Iwasa et al. has been analysed in more detail by Serra and co-workers (Serra, 2006; Serra and Haccou, 2007; Sagitov and Serra, 2009). These authors have thus considered the process of evolutionary escape as a random search on a genotype space modelled by a hypercube: individuals concentrate in a given non-escape genotype and they must reach a well-adapted genotype (the so-called escape genotype) before the population undergoes extinction. An alternative escape mechanism has been proposed in Alarcon and Jensen (2010) whereby escape is achieved by means of a growth-restricted (quiescent) phenotype that is insensitive to the selective pressure (e.g. a drug). This escape mechanism is relevant in cancer treatment of hypoxic tumours (Alarcon et al., 2005; Brikci et al., 2008; Bristow and Hill, 2008) and drug resistance in bacterial populations which exhibit persistence (Balaban et al., 2004; Lewis, 2007).

While the assumption that point mutations drive evolutionary escape is preserved in our study, we investigate whether considering the more realistic mechanism whereby selective pressures act on phenotypes rather than genotypes alters the properties of evolutionary escape in significant ways. To this end we describe evolutionary escape in terms of a population dynamic that accounts for the genotype–phenotype map. This modification alters the approach proposed by Iwasa et al. in two relevant aspects. First, due to evolved robustness in populations with genotype–phenotype map (Wagner, 1996; Ciliberti et al., 2007, 2007; Wagner, 2007, 2008, 2008; Jaeger and Monk, 2014), not every gene mutation necessarily generates a new phenotype. As a consequence, many gene mutations are neutral as far as the evolutionary escape process is concerned. Furthermore, it has been shown that the topology of genotype–phenotype networks is far from that of the hypercube lattice assumed by Aguirre et al. (2011) and Ibáñez-Marcelo and Alarcon (2014). In fact, we have recently shown that the corresponding phenotype network exhibits the small-world phenomenon and that, as a consequence, accelerated evolvability (relative to that of a system with no genotype–phenotype map) may emerge. The question naturally arises as to whether these properties, i.e. phenotypic robustness and evolvability typical of genotype–phenotype networks, have an influence on the process of evolutionary escape. To address this issue, we apply a general theory, based on multitype branching processes (Kimmel and Axelrod, 2002), to compute the evolutionary dynamics and probabilities of escape which takes into account the structure of the genotype–phenotype space.

The structure and properties of systems with genotype–phenotype maps have been studied by considering several model systems (Wagner, 2012): RNA, circuits of gene regulation and metabolic networks. In the RNA model of the genotype–phenotype map (Fontana and Schuster, 1998), the *genotype* of each RNA molecule is its sequence of nucleotides. There are four such nucleotides, so for sequences of length  $L$ , the size of the genotype space is  $4^L$ . The folded structure of an RNA sequence, which is a proxy for its *phenotype* (although it still lies far from defining its function), is determined by the sequence (genotype) in a many-to-one way, i.e. many different genotypes have the same associated phenotype. Such non-uniqueness has led to the concept of the neutral network, first introduced in Lipman and Wilbur (1991) and Schuster et al. (1994), which is defined as the network whose nodes correspond to genotypes, all with the same phenotypes, with edges between those nodes which differ by only one nucleotide (Wagner, 2007). This concept has been used extensively in the study of the genotype–phenotype map, in particular, those issues regarding its evolutionary properties, such as the role of phenotypic robustness in evolvability and adaptation (Wagner, 2011, 2012). Recently, the topology of the RNA genotype–phenotype space, composed by an intermingled set of neutral networks, has been analysed (Aguirre et al., 2011).

Gene regulatory networks (GRNs) have also been extensively used as models of the genotype–phenotype map, in particular several variants of the model of phenotype plasticity originally introduced by Wagner (1996). These models are dynamical systems for the expression levels of the corresponding genes and are characterised by two elements: a matrix whose entries specify the character of the interaction between two genes (usually, activation or inhibition) and, possibly, the intensity of such interaction, and a series of rules for the time evolution of the expression levels of the genes involved. The entries of the corresponding matrix are defined as the genotype of the GRN. The associated phenotype is the steady-state gene expression yielded by the dynamics. There are many such genotypes associated to the same phenotype, which allows to extend the concept of neutral network to GRNs, where nodes correspond to different matrices (producing the same steady-state) and links exist between nodes if the corresponding matrices differ only in one regulatory interaction. GRNs have been used to study phenotype plasticity (Wagner, 1996), robustness and innovation in circuits of gene regulation (Ciliberti et al., 2007, 2007), and canalisation (Siegal and Bergman, 2002; Bergman and Siegal, 2003), among other issues.

Metabolic networks are a third class of systems that have been used to assess properties regarding robustness and innovation (Ndifon et al., 2009; Rodrigues and Wagner, 2009; Samal et al., 2010; Rodrigues and Wagner, 2011). They are formed by thousands of enzyme-catalysed chemical reactions. These networks are responsible for supplying cells with energy (i.e. ATP) and the molecular building blocks that cells need to grow. The *genotype* space for this system consists of the space of all the possible metabolic networks, whereas the *phenotype* corresponds to the secondary metabolites the metabolic network is able to synthesise, the molecules they can use as energy sources, the ability to detoxify certain waste products, etc. (Wagner, 2012). Innovations in these aspects not always appear as the result of gene mutations that give rise to new enzymes. They can also arise through novel combinations and utilisation of existing elements.

Genotype–phenotype networks have been extensively used and analysed in RNA and GRN models of the genotype–phenotype map. These are networks whose set of nodes corresponds to the set of (viable) genotypes (e.g. each nucleotide sequence that yields a properly folded molecule). A link between a pair of genotypes exist if they are separated by one single mutation (e.g. an RNA molecule is linked to all its (viable) single-point mutants). The ensemble of genotypes associated to the same phenotype form its neutral network. In Ibáñez-Marcelo and Alarcon (2014), we added to this picture the so-called phenotype nodes which correspond to the set of (viable) phenotypes. Links between genotype and phenotype nodes exist if the genotype node belongs to the neutral network of that particular phenotype.

Our aim is to extend the theory of evolutionary escape by analysing the effects on the probability of escape and the escape rate of considering that the evolutionary dynamics occurs on a complex genotype–phenotype network rather than on a regular hypercube. This paper is organised as follows. Section 2 is devoted to a detailed description of our model and a summary of the mathematical background involved in its analysis. A full account of the mathematical apparatus is included in the Supplementary Materials. In Section 3, we report the results of our analysis and our main findings. Finally, in Section 4, we present our conclusions and discuss our results as well as future directions for further research.

## 2. Mathematical model

The classical escape model (Iwasa et al., 2003, 2004; Serra, 2006; Serra and Haccou, 2007; Sagitov and Serra, 2009) can be summarised as follows. Each of the  $2^n$  nodes of an  $n$ -dimensional hypercube is assumed to represent a genotype. Fitness values,

represented here by the reproductive ratio,  $R$ , defined as the average number of offspring per individual, are assigned directly to genotypes. The population is assumed to be concentrated in one genotype which, prior to the change in selective pressure (as a consequence of e.g. the administration of a drug), was well adapted. Upon initiation of treatment, the initial genotype becomes ill-adapted to the new selective pressure, i.e. its reproductive ratio becomes  $R < 1$ . To avoid extinction the population needs to start a random, mutation driven search on the genotype hypercube, until it finds an *escape genotype*, i.e. a genotype such that its reproductive number satisfies  $R > 1$ . The reproductive number of all genotypes other than the escape genotype are such that  $R < 1$ . This implies that only the escape genotype has a positive probability of long-term survival (Kimmel and Axelrod, 2002).

The random search on the genotype hypercube is performed by an evolutionary dynamics that takes the form of a multi-type Galton–Watson branching process with mutation (Iwasa et al., 2003, 2004; Serra, 2006; Serra and Haccou, 2007; Sagitov and Serra, 2009). Upon proliferation, each cell has a certain probability of mutating, the mutation rate  $\nu$ , which allows the population to spread over the genotype hypercube until escape is achieved, by sequentially moving between genotypes until the escape genotype is reached, or extinction eventually occurs.

For reference, a summary of the parameters and their description used in our model is given in Table 1.

### 2.1. Genotype–phenotype network

We extend the basic framework for analysing evolutionary escape by introducing two modifications. The first one concerns the topology of the space on which the evolutionary dynamical process occurs. We assume that the space on which the escape process performs its random search is not a regular hypercube (Iwasa et al., 2003, 2004; Serra, 2006; Serra and Haccou, 2007; Sagitov and Serra, 2009), but a complex genotype–phenotype network (Ciliberti et al., 2007, 2007; Aguirre et al., 2011; Ibáñez-Marcelo and Alarcon, 2014).

In Ibáñez-Marcelo and Alarcon (2014), we have formulated an evolutionary model of the genotype–phenotype network associated to gene regulatory networks (GRNs). A summary of this model is presented here. The reader is referred to the Supplementary Materials for a fully detailed description. The definition of the genotype–phenotype map is based on the idea, proposed by Stuart Kauffman, that GRNs are dynamical systems and phenotypes (e.g. differentiated states) correspond to the stable attractors of these

dynamical systems (Kauffman, 1993). Within this framework, we represent GRNs as graphs (Wagner, 1996; Siegal and Bergman, 2002; Bergman and Siegal, 2003; Ciliberti et al., 2007, 2007) and we consider the genotype as the pair  $\mathcal{G} = (G, g(0))$ .  $G = (g_{ij})$  is the weighted adjacency matrix accounting for the interaction between genes, i.e. how a gene product affects the (in)activation of all other genes:  $g_{ij} = \pm 1$  if there exists a link between nodes (genes)  $i$  and  $j$ , and  $g_{ij} = 0$ , otherwise. Positive (negative) interactions correspond to activating (inhibitory) interactions between genes. The vector  $g(0)$  corresponds to the initial pattern of gene expression, which can be interpreted as heritable genetic information: the components of  $g(0) = (g_i(0))$  are the states (active or inactive) of each gene when new cells are born. The phenotype is defined as the steady-state of the dynamical system defined by the following set of rules:

1. At  $t=0$ , that is, at the time of birth of each cell, the initial condition  $g(t=0) = g(0)$  is set.
2. At each time step, and for each gene  $i$ , the value of the quantity  $I_i(t)$ :

$$I_i = \sum_j g_{ji} g_j, \text{ where} \quad (1)$$

is determined

3. We determine the state of each gene at step  $t+1$  according to:
 
$$\begin{cases} g_i(t+1) = 1, & \text{if } I_i(t) \geq 0 \\ g_i(t+1) = -1, & \text{if } I_i(t) < 0 \end{cases}$$

4. Steps 2 and 3 are repeated until  $t = T \gg 1$ . The phenotype corresponding to the genotype  $\mathcal{G} = (G, g(0))$ ,  $\phi(\mathcal{G})$ , is defined by  $\phi(\mathcal{G}) = g(T)$ .

We further set forth conditions to discard genotypes which give rise to *unviable* phenotypes. Our viability conditions are related by those imposed by Siegal and Bergman (2002), Bergman and Siegal (2003) (see Ibáñez-Marcelo and Alarcon, 2014 and Supplementary Materials for more details).

Based on this definition of the genotype–phenotype map and the viability conditions, which act as a selecting pressure against genotypes leading to unviable phenotypes, we have proposed a model which generates the corresponding genotype–phenotype network (Ibáñez-Marcelo and Alarcon, 2014). Within this network genotypes and phenotypes are represented by nodes of different types. Edges between nodes are also of two types. Edges between two genotype nodes correspond to *viable* gene mutations, i.e. mutations that generate a genotype associated to a viable phenotype. An edge between a genotype node,  $\mathcal{G}_i$  and a phenotype node,  $\phi_j$ , exists if and only if  $\phi(\mathcal{G}_i) = \phi_j$ . In this formulation the neutral network associated to a phenotype,  $\phi_j$ , is the set of its neighbours, i.e. all those genotypes such that  $\phi(\mathcal{G}) = \phi_j$ . Neutral networks corresponding to different phenotypes may be connected through genotype–genotype edges, i.e. via viable mutations producing two different (viable) phenotypes.

This pseudo-bipartite description of the genotype–phenotype network allows us to define several properties of the genotype–phenotype map in topological terms, in particular those which are relevant for the escape process, namely, robustness and evolvability (Ibáñez-Marcelo and Alarcon, 2014). We have characterised phenotypic robustness by means of the clustering coefficient of the phenotype nodes, which is associated to point mutations which do not change the phenotype (Ibáñez-Marcelo and Alarcon, 2014). In order to characterise evolvability, we have studied the phenotype network, defined as the corresponding one-mode projection of the genotype–phenotype network, i.e. we have defined a network whose nodes represent the (viable) phenotypes. An edge exists between two phenotypes,  $\phi_i$  and  $\phi_j$ , if there exists at least one path of minimal length between  $\phi_i$  and  $\phi_j$  in the full

**Table 1**  
Description of parameters.

Parameter	Description
$R$	Reproduction rate
$R_E$	Escape phenotype reproduction rate
$\nu$	Mutation rate
$N_i(t)$	Number of cells with genotype $\mathcal{G}_i$ at time $t$
$N_E(t)$	Total number of cells in the escape phenotype $\phi_E$
$B$ class graph	Pseudo-bipartite graph generated by model Ibáñez-Marcelo and Alarcon (2014),
$H$ class graph	Artificial genotype–phenotype graph, where genotype space is modelled as an hypercube
$\lambda$	Birth probability in genotypes $\mathcal{G}_i$ such that, $\phi(\mathcal{G}_i) \neq \phi_E$
$\sigma$	Death probability in genotypes $\mathcal{G}_i$ such that, $\phi(\mathcal{G}_i) \neq \phi_E$
$\lambda_E$	Birth probability in genotypes $\mathcal{G}_i$ such that, $\phi(\mathcal{G}_i) = \phi_E$
$\sigma_E$	Death probability in genotypes $\mathcal{G}_i$ such that, $\phi(\mathcal{G}_i) = \phi_E$
$P_S(t)$	Survival probability at time $t$
$P_E(t)$	Escape probability at time $t$
$N$	Initial population to generate $B$ graphs using model Ibáñez-Marcelo and Alarcon (2014)
$n$	Number of genotypes
$\tau_E$	Average escape time



genotype–phenotype network. Since there need not be a unique such path between  $\phi_i$  and  $\phi_j$ , the phenotype network is weighted: the weight of each edge is given by the number of minimal paths between the corresponding phenotypes. Evolvability, i.e. the ability of the system to explore new phenotypes, is then characterised in terms of the distribution of connected components in the phenotype network and the emergence of giant connected component which allows global navigation between phenotypes (Ibáñez-Marcelo and Alarcon, 2014).

This topological definition of evolvability allows us to characterise the robustness properties of evolvability, which is defined in terms of the robustness against attack (i.e. edge removal) of the giant connected component. Using this model, we have determined that phenotypic robustness and cryptic genetic variation are key to the integrity of evolvability.

We have further showed (Ibáñez-Marcelo and Alarcon, 2014) that the phenotype network exhibits the small-world phenomenon, which implies that in this type of evolutionary system the rate of adaptability appears to be enhanced. Our aim in this study is to ascertain whether these topological properties of the genotype–phenotype network, insofar as they affect the evolvability of the system, alter the ability for evolutionary escape predicted on a genotype hypercube.

In order to proceed further, we consider two classes of graphs (see Fig. 1):

- **B:** Genotype–phenotype networks as modelled in Ibáñez-Marcelo and Alarcon (2014) (see also the Supplementary Materials).
- **H:** An artificial genotype–phenotype graph where the genotype space is given by a hypercube. Phenotypes are assigned randomly to genotypes so that the phenotype degree distribution, i.e. the probability distribution of the number of genotypes bearing a given phenotype, is the same as that resulting from the multiscale model in Ibáñez-Marcelo and Alarcon (2014).

## 2.2. Population dynamics

A further modification we introduce with respect to the original model by Iwasa et al. (2003) is the fact that we now associate fitness to phenotypes rather than genotypes, i.e. the value of the reproduction number depends on the phenotype: different genotypes which exhibit the same phenotype have the same reproduction number.

In this section we summarise the methodology used to compute the escape probability. Within the present framework, the escape probability is defined as the probability of reaching the

neutral network of the escape phenotype,  $\phi_E$ , which we assume to have a reproduction number  $R_E \rightarrow \infty$ . The reproduction number of every phenotype  $\phi_i \neq \phi_E$  is assumed to be  $R_i < 1$ . The population undergoes a branching process with mutation which allows to explore the genotype–phenotype network. Under the assumption that the reproduction number of the escape phenotype is such that  $R_E \rightarrow \infty$ , the escape probability is the probability of the population to reach the neutral network of the escape phenotype before extinction occurs. We focus on the comparison between the escape process on different genotype–phenotype: graphs of classes **B**, i.e. complex genotype–phenotype networks, or **H**, where the genotype space is a regular hypercube (see Fig. 1).

In order to model our evolutionary dynamics on **B**- and **H**-class networks, we follow the previous literature on the subject (Iwasa et al., 2003, 2004; Serra, 2006; Serra and Haccou, 2007; Sagitov and Serra, 2009) and consider a Galton–Watson multi-type branching process (Kimmel and Axelrod, 2002). The process takes place on the genotype network and each type corresponds to a different genotype. When we refer to the population of type  $i$  at generation  $t$ ,  $N_i(t)$ , we mean the number of cells with genotype  $\mathcal{G}_i$  at time  $t$ . Furthermore, we define

$$N_E(t) = \sum_{i \in \langle \phi_E \rangle} N_i(t)$$

as the total population of the escape phenotype. The sum in the above expression is done over all the genotypes belonging to the neutral network of the escape phenotype  $\langle \phi_E \rangle$ .

The process is assumed to start with a clonal population, i.e. the whole initial population concentrated in one single genotype,  $\mathcal{G}_0$ , such that  $\phi(\mathcal{G}_0) \neq \phi_E$ . The evolutionary dynamics is characterised by two parameters: the birth probability,  $\lambda$ , and the mutation rate,  $\nu$ . Whereas the latter is assumed to be independent on genotype/phenotype of the cell,  $\lambda$  is assumed to be dependent on phenotype, i.e.  $\lambda = \lambda(\phi_i)$ . From the point of view of the evolutionary dynamics, this implies that all genotypes associated to the same phenotype have the same birth probability. The death probability,  $\sigma$ , is given by  $\sigma = 1 - \lambda$  and it therefore depends on the phenotype. We further define the reproduction ratio (Iwasa et al., 2003)  $R(\phi_i) = \lambda(\phi_i)/\sigma(\phi_i)$ . For simplicity, we assume that  $\lambda(\phi_i) = \lambda = \text{cst.}$  for all genotypes such that  $\phi(\mathcal{G}_i) = \phi_i \neq \phi_E$ . We assume that  $\lambda \ll \lambda_E$  where  $\lambda_E$  is the birth probability of those genotypes such that  $\phi(\mathcal{G}_i) = \phi_E$ . In fact, we consider  $R(\phi_E) \rightarrow \infty$ , so that once the system reaches an escape genotype, the survival probability  $P_S \rightarrow 1$ .

The evolutionary dynamics is defined as follows. At each time step (generation) each individual can:

- Reproduce with no mutation with probability  $\lambda(1 - \nu)^2$ .
- Reproduce with asymmetrical mutation, i.e. one of the descendants mutates, the other retains the genotype of its mother cell. This event occurs with probability  $2\lambda\nu(1 - \nu)$ .
- Reproduce with symmetric mutation, i.e. both descendants mutate, which occurs with probability  $\lambda\nu^2$ .
- Die with probability  $\sigma = 1 - \lambda$ .

This dynamic is iterated until either an escape genotype is reached, upon which escape is assumed to occur with probability one, or the population undergoes extinction.

In order to proceed further, we recall the following definitions regarding multi-type Galton–Watson branching processes (Kimmel and Axelrod, 2002):

- We define  $f_i(s_1, \dots, s_n; t) = \mathbb{E}(s_1^{N_1(t)} \cdot s_2^{N_2(t)} \dots s_n^{N_n(t)} | N_i(0) = 1, N_j(0) = 0, \forall j \neq i)$  as the generating function of probability of the population to be  $(N_1(t), \dots, N_n(t))$  at time conditioned to the initial condition of the system to consist of a single individual of type  $i$ , i.e.  $N_j(t=0) = \delta_{ij}$  for  $j = 1, \dots, n$ . We further define  $\vec{s} = (s_1, s_2, \dots, s_n)$ . Each component,  $s_i$ , satisfies  $0 \leq s_i \leq 1 \quad \forall i$ .

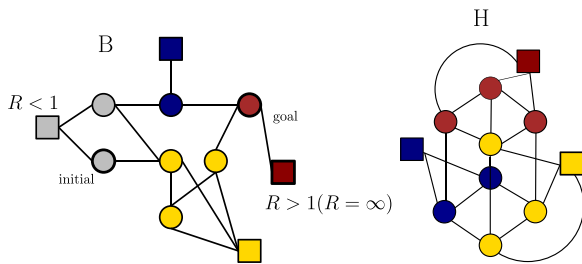


**Fig. 1.** Schematic representation of the two types of networks considered in this paper: plot (a) corresponds to a pseudo-bipartite genotype–phenotype graph, **B**, constructed according to the model (Ibáñez-Marcelo and Alarcon, 2014), whereas (b) corresponds to a hypercube graph, **H**. In both plots, phenotype nodes are represented as squares and genotype nodes as circles. Each colour represent a different phenotype and their associated genotypes. Edges between nodes allow identify map between genotype–phenotype and feasible mutations between genotypes. Heavier strokes in some nodes indicates the initial genotype, characterised by a reproduction number such that  $R < 1$ , i.e. bound to long-term extinction, and the goal or escape genotype, which we consider to have a reproduction number  $R = \infty$ . In other words, we assume that once the system reaches a genotype corresponding to the escape phenotype, the extinction probability is vanishingly small. (For interpretation of the references to colour in this figure caption, the reader is referred to the web version of this paper.)

- We consider the progeny probability generating function,  $F_i(\vec{s})$ , which is defined as the generating function corresponding to the probability distribution of the number of offspring of a cell with genotype  $G_i$ .

The dynamics of a multi-type Galton–Watson process is described by two (equivalent) functional equations, namely, the forward equation

$$\vec{f}(\vec{s}, t+1) = \vec{F} \circ \vec{F} \circ \dots \circ \vec{F}(\vec{s}) = \vec{F}(\vec{F}(\vec{F} \dots \vec{F}(\vec{s}))) \quad (2)$$

where the progeny probability generating function is composed with itself  $t+1$  times, and the backward equation:

$$\vec{f}(t+1) = \vec{f}(\vec{F}(\vec{s}), t) \quad (3)$$

where  $\vec{f} = (f_1, \dots, f_n)$  and  $\vec{F} = (F_1, \dots, F_n)$ .

According to our model evolutionary dynamics, the progeny generating function of a non-escape genotype  $G_i$ , i.e.  $\phi(G_i) \neq \phi_E$ ,  $F_i(\vec{s})$  is given by

$$F_i(\vec{s}) = \sigma + \lambda(1-\nu)s_i^2 + \sum_j 2\lambda\nu(1-\nu)\frac{a_{ij}}{d_i}s_i s_j + \sum_{j,k} \lambda\nu^2 \frac{a_{ij}a_{ik}}{d_i^2} s_j s_k \quad (4)$$

where  $A = (a_{ij})$  is the adjacency matrix of genotype graph (defined as a sub-graph of the genotype–phenotype network) and  $d_i$  is the degree of genotype  $i$  in the genotype network.

On the other hand, the progeny generating function of an escape genotype, i.e.  $\phi(G_i) = \phi_E$ , is given by

$$F_i(\vec{s}) = s_i. \quad (5)$$

In order to simplify notation we will define for non escape genotypes, we further define the matrix  $D = (d_{ij} = d_i \delta_{ij})$  and denote  $\vec{1} = \begin{pmatrix} 1 \\ \vdots \\ 1 \end{pmatrix}$ . In terms of the matrices  $A$  and  $D$ ,  $\vec{F}(\vec{s})$  can be re-written as

$$\begin{aligned} \vec{F} &= \sigma \cdot \vec{1} + \lambda(1-\nu)s^2 \odot \vec{s} + 2\lambda\nu(1-\nu)(D^{-1}A \cdot \vec{s}) \\ &\odot \vec{s} + \lambda\nu^2(D^{-1}A \cdot \vec{s}) \odot (D^{-1}A \cdot \vec{s}) = \sigma \cdot \vec{1} + \lambda(B \cdot \vec{s}) \\ &\odot (B \cdot \vec{s}) \end{aligned} \quad (6)$$

where  $\odot$  denotes the component-to-component product and  $B = \nu D^{-1}A + (1-\nu)Id$  with  $Id$  equal to the identity matrix.

**Escape probability at time  $t$ ,  $P_E(t)$ :** The generating function  $\vec{f}(\vec{s}, t)$  encodes all the information of the process, in particular, that pertaining to the escape probabilities. To calculate the escape probability, we need to fix the initial genotype and the escape phenotype. The escape phenotype has associated all those genotypes such that  $\phi(G_i) = \phi_E$ . In order to proceed further, we define

$$\vec{\theta}_0 := (1, 1, 1, \dots, 0, 0)$$

where

$$(\vec{\theta}_0)_i = \begin{cases} 0 & \text{if } \phi(G_i) = \phi_E \\ 1 & \text{otherwise} \end{cases} \quad (7)$$

Since  $\vec{\theta}_t := f(\vec{\theta}_0, t)$ , then  $\vec{\theta}_t$  satisfies

$$(\vec{\theta}_t)_i = P(N_E(t) = 0 | N_i(0) = 1, N_j(0) = 0 \quad \forall j \neq i),$$

that is the probability of no individuals to have reached the escape phenotype at time  $t$ , assuming that the population is initially composed by one individual of type  $i$ . Then,

$$\begin{aligned} (\vec{\theta}_t)_i &= \mathbb{E}(s_1^{N_1(t)} \cdot s_2^{N_2(t)} \dots s_n^{N_n(t)} | N_i(0) = 1, N_j(0) = 0, \forall j \neq i) \Big|_{\vec{s} = \vec{\theta}_0} \\ &= P(N_{k_1}(t) = n_{k_1}, \dots, N_{k_l}(t) = n_{k_l} | N_i(0) = 1, N_j(0) = 0, \forall j \neq i) \\ &= P(N_E(t) = 0 | N_i(0) = 1, N_j(0) = 0, \forall i \neq j) \end{aligned} \quad (8)$$

where  $k_i, i = 1, \dots, l$  refer to all the genotypes belonging to the

neutral network of the escape phenotype:  $\phi(G_{k_i}) = \phi_E$ . The quantities  $(\vec{\theta}_t)_i$  are obtained by iteration of Eq. (6):

$$\vec{\theta}_{t+1} = \sigma \cdot \vec{1} + \lambda(B \cdot \vec{\theta}_t) \odot (B \cdot \vec{\theta}_t) \quad (9)$$

The quantities  $(\vec{\theta}_t)_i$  are closely related to the escape probability at time  $t$ . Consider the probability of not reaching the escape phenotype at time  $t-1$ ,  $P(N_E(t-1) = 0)$ , which can be expressed as

$$\begin{aligned} P(N_E(t-1) = 0) &= P(N_E(t-1) = 0 | N_E(t) > 0)P(N_E(t) > 0) + P(N_E(t-1) \\ &= 0 | N_E(t) = 0)P(N_E(t) = 0) \end{aligned}$$

Recalling that  $P(N_E(t-1) = 0) = (\vec{\theta}_{t-1})_i$  and

$$P(N_E(t-1) = 0 | N_E(t) = 0)P(N_E(t) = 0) = P(N_E(t) = 0) = (\vec{\theta}_t)_i,$$

we have that

$$(\vec{\theta}_{t-1})_i - (\vec{\theta}_t)_i = P(N_E(t-1) = 0 | N_E(t) > 0)P(N_E(t) > 0),$$

which, in turn, implies that the probability of reaching the escape phenotype precisely at time  $t$ , or, in other words, the escape time probability,  $P(N_E(t-1) = 0 \wedge N_E(t) > 0 | N_i(0) = 1, N_j(0) = 0, \forall i \neq j)$  is given by

$$\begin{aligned} P_E(t) &= P(N_E(t-1) = 0 \wedge N_E(t) > 0 | N_i(0) = 1, N_j(0) = 0, \forall i \neq j) \\ &= (\vec{\theta}_{t-1} - \vec{\theta}_t)_i \end{aligned} \quad (10)$$

Since  $\mathbb{E}(N_E(t))$  is an increasing function of  $t$ , it follows that

$$P(N_E(t) = 0 | N_i(0) = 1, N_j(0) = 0, \forall i \neq j) \geq P(N_E(t+1) = 0 | N_i(0) = 1, N_j(0) = 0, \forall i \neq j),$$

and therefore we have that  $(\vec{\theta}_t)_i \geq (\vec{\theta}_{t+1})_i$ . This inequality has two important consequences, namely, (i)  $(\vec{\theta}_{t-1} - \vec{\theta}_t)_i \geq 0$ , which guarantees that the escape probability at time  $t$  (Eq. (10)) is well-defined (i.e. non-negative), and (ii)  $\vec{\theta}_t$  converges to  $\vec{\theta}_\infty$  as  $t \rightarrow \infty$ .

**Escape probability,  $P(N_E(\infty) > 0)$ .** From the above results, we are able to compute the asymptotic escape probability,  $P(N_E(\infty) > 0)$ , in terms of the escape time probability  $P_E(t)$ :

$$P(N_E(\infty) > 0) = 1 - (\vec{\theta}_\infty)_i = \sum_t P_E(t) \quad (11)$$

where  $\vec{\theta}_\infty = \lim_{t \rightarrow \infty} \vec{\theta}_t$  satisfies

$$\vec{\theta}_\infty = \sigma \cdot \vec{1} + \lambda(B \cdot \vec{\theta}_\infty) \odot (B \cdot \vec{\theta}_\infty) \quad (12)$$

Using Eq. (11)  $P(N_E(\infty) > 0)$  can be efficiently calculated as a cumulative probability, rather than by directly solving Eq. (12) (Iwasa et al., 2003). In practice the (infinite) summatory in Eq. (11) is only summed until it barely changes anymore.

**Recursive calculation of the escape probability:** We consider the following recursion in order to obtain escape probability at time  $t$ . We consider the quantity  $\vec{1} - \vec{\theta}_t$ . By defining  $\vec{\psi}_t = \vec{1} - \vec{\theta}_t$ , Eq. (9) leads to

$$\vec{1} - \vec{\psi}_{t+1} = \sigma \cdot \vec{1} + \lambda(B \cdot (\vec{1} - \vec{\psi}_t)) \odot (B \cdot (\vec{1} - \vec{\psi}_t)) \quad (13)$$

After some algebra, we obtain the following recursion equation:

$$\vec{\psi}_{t+1} = 2\lambda B \vec{\psi}_t - \lambda(B \vec{\psi}_t \odot B \vec{\psi}_t) \quad (14)$$

The recursion equation (14) is numerically better behaved than Eq. (9).

### 3. Results

In this section, we report the results of our comparative analysis of evolutionary escape on  $B$  and  $H$  genotype–phenotype

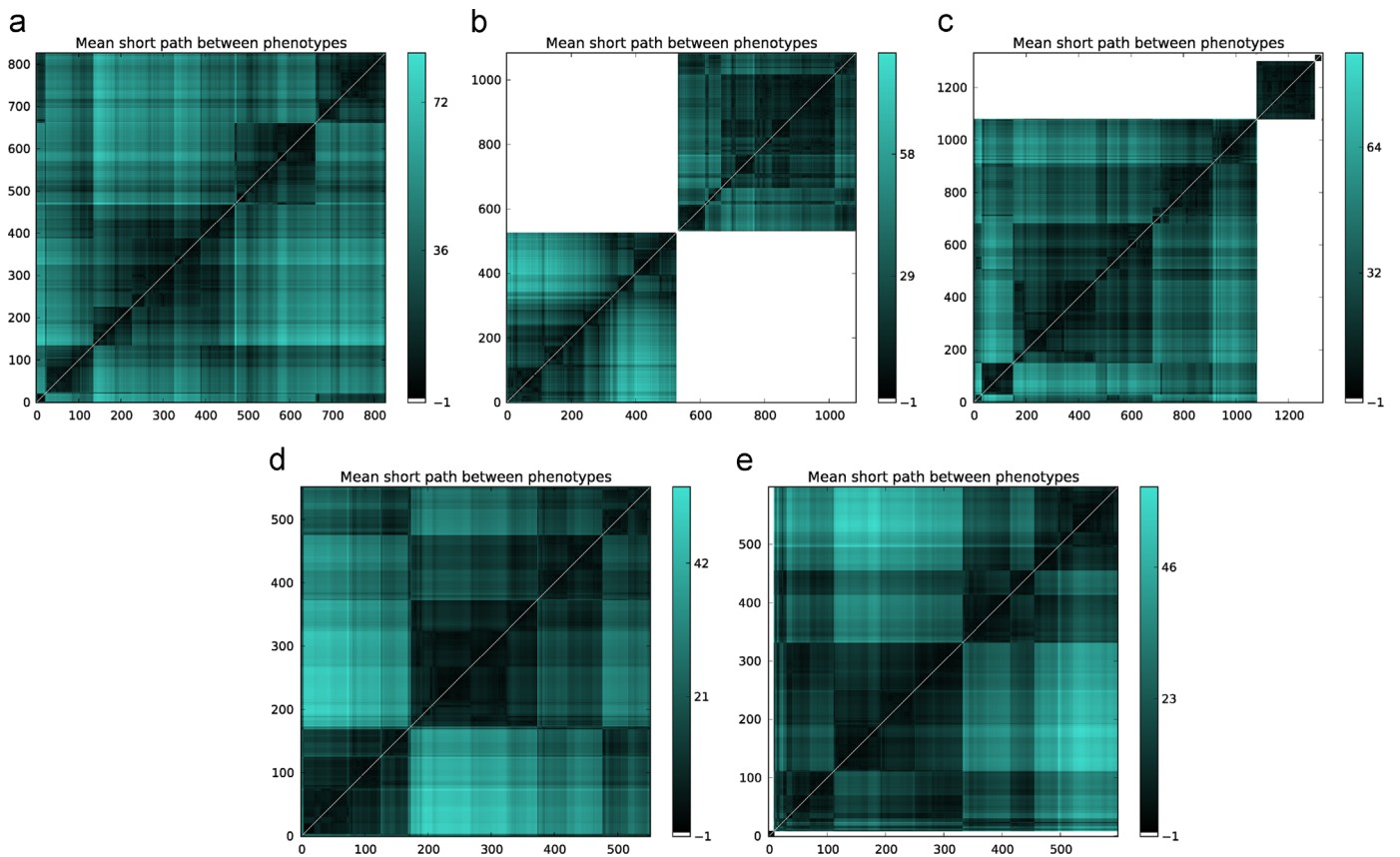


**Fig. 2.** Mean short path between phenotypes ordered by clusters. Different graph structures are observed. White corresponds to no path between two phenotypes, black or really dark means distance from 1 to 10 (approx), from black to turquoise length path increases. These are graph with viability 7 and GRN modelled as Strogatz–Watts graph with parameter  $p=0.1$ . Initial genotypes,  $N=50$  and for (a)–(c) mutation rate is  $\nu=0.3$ , (d) and (e)  $\nu=0.01$ . See the Supplementary Materials for a full account of the details of the model used to generate these networks.

graphs. We first focus on structural properties of both types of genotype–phenotype networks, in particular, those characterising the distance between phenotypes, which is an essential property of the networks affecting evolutionary escape. We then proceed to analyse the dynamics of escape on both types of networks, according to the model presented in Section 2.2. We first focus on the steady-state ( $t \rightarrow \infty$ ) properties of the escape probability. We then move on to the study of dynamical properties of evolutionary escape as characterised by several metrics, namely, the escape time probability, the average escape time, and the escape time probability conditioned to escape.

### 3.1. Connectivity structure of genotype–phenotype networks

As a first step towards understanding the properties of the evolutionary escape phenomenon on genotype–phenotype networks, we investigate the connectivity structure of our  $B$  graphs, as this structure directly affects the properties of random walks on networks (Lambiotte et al., 2009; Delvenne et al., 2010; Schaub et al., 2010) and is therefore related to the escape dynamics.

In order to proceed with our analysis, we start by investigating the distance between phenotypes on  $B$ -networks. An estimation of this quantity can be obtained via the average shortest path length between phenotypes which is computed as follows. For each genotype–phenotype graph, we consider its giant connected component (GCC). More specifically, we consider the genotype one-mode projection of the GCC. Note that, as we are not considering the phenotype nodes, the genotype one-mode projection of the GCC is not necessarily connected. Once this one-mode projection has been determined, we compute the shortest path between every pair of genotypes, which in

turn allows us to compute the average distance between phenotypes by averaging over the distances between genotypes belonging to two given phenotypes. In order to visualise our results of the network we make a cluster hierarchy, using a method implemented in Python: `scipy.cluster.hierarchy.linkage`. Several examples of this cluster analysis are shown in Fig. 2, where we have colour-coded the different phenotypes according to the distance between them: darker (lighter) colour is associated to smaller (bigger) average shortest path between corresponding phenotypes. White indicates that there is no path between phenotypes (i.e. the average shortest path is of infinite length).

Our analysis shows that genotype–phenotype networks exhibit a high degree of heterogeneity. We distinguish between two cases (see Supplementary Electronic Materials): genotype–phenotype networks associated to large populations (i.e.  $\nu N > 1$ ) and genotype–phenotype networks corresponding to small populations (i.e.  $\nu N < 1$ ). The evolutionary dynamics of populations in these two limits is fundamentally different: whereas populations with high mutation rates ( $\nu N > 1$ ) are likely to be polymorphic at any given generation, with individuals accumulating over time in regions of the genotype space with genotypes characterised by high mutational robustness, populations with low mutation rate ( $\nu N < 1$ ) tend to be monomorphic with individuals performing a random walk that samples the genotype network uniformly (Wagner, 2008). These properties are reflected in our analysis: we observe that those genotype–phenotype networks associated to  $\nu N > 1$  are more likely to exhibit a structure where separated communities of phenotypes, i.e. genotype–phenotype networks where disjoint subsets phenotypes emerge (see Fig. 2(b) and (c)), thus enabling for polymorphic populations to appear. Such disjoint subsets of

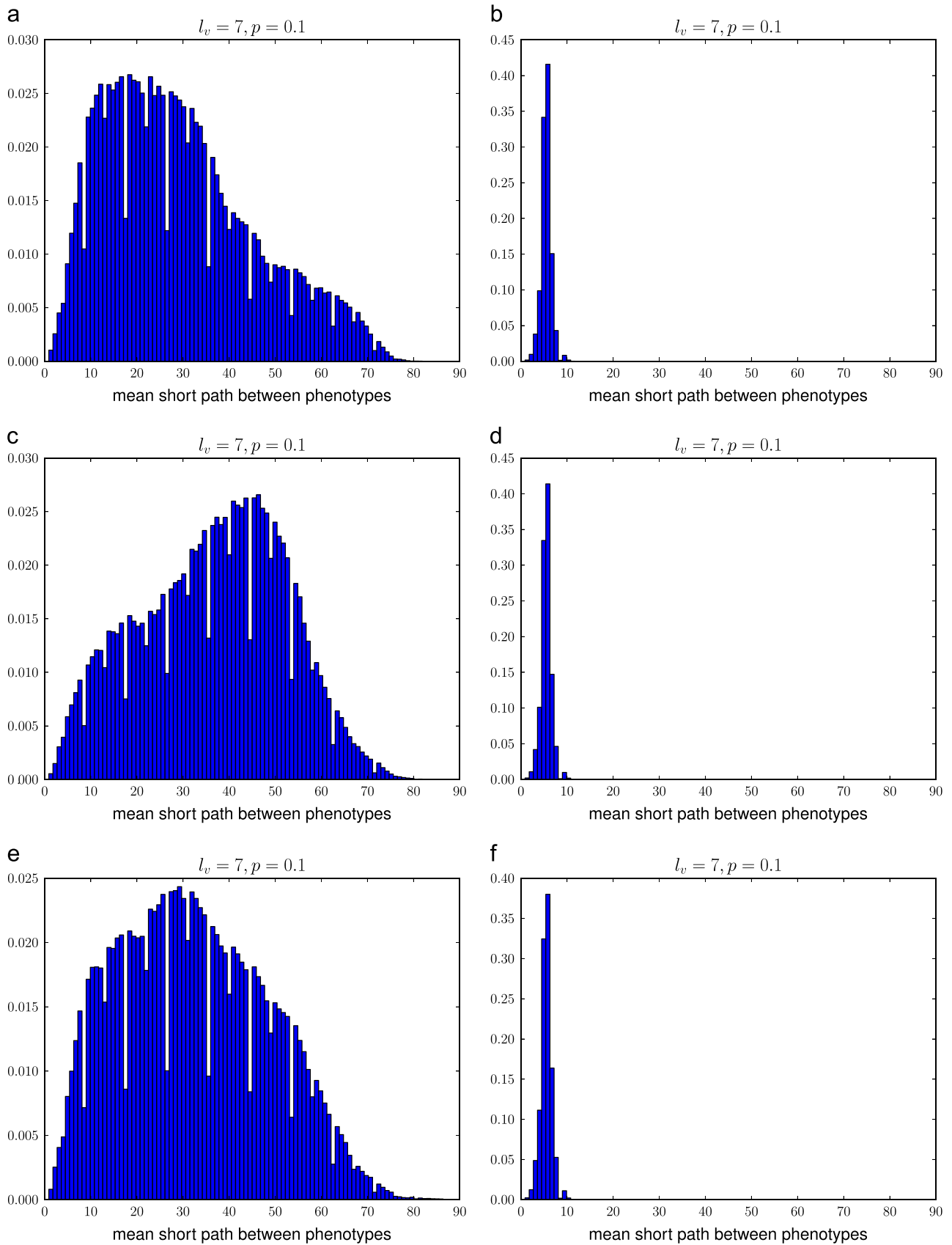


**Fig. 3.** Series of plots showing the normalised histograms for the average distance between phenotypes associated to the data corresponding to the genotype–phenotype graphs shown in Fig. 2 (a)–(c),  $N_v = 1.5$  (plots (a), (c), and (e)), and the normalised histograms for the corresponding  $H$ -type genotype–phenotype maps (plots (b), (d), and (f)). See the Supplementary Materials for a full account of the details of the model used to generate these networks.



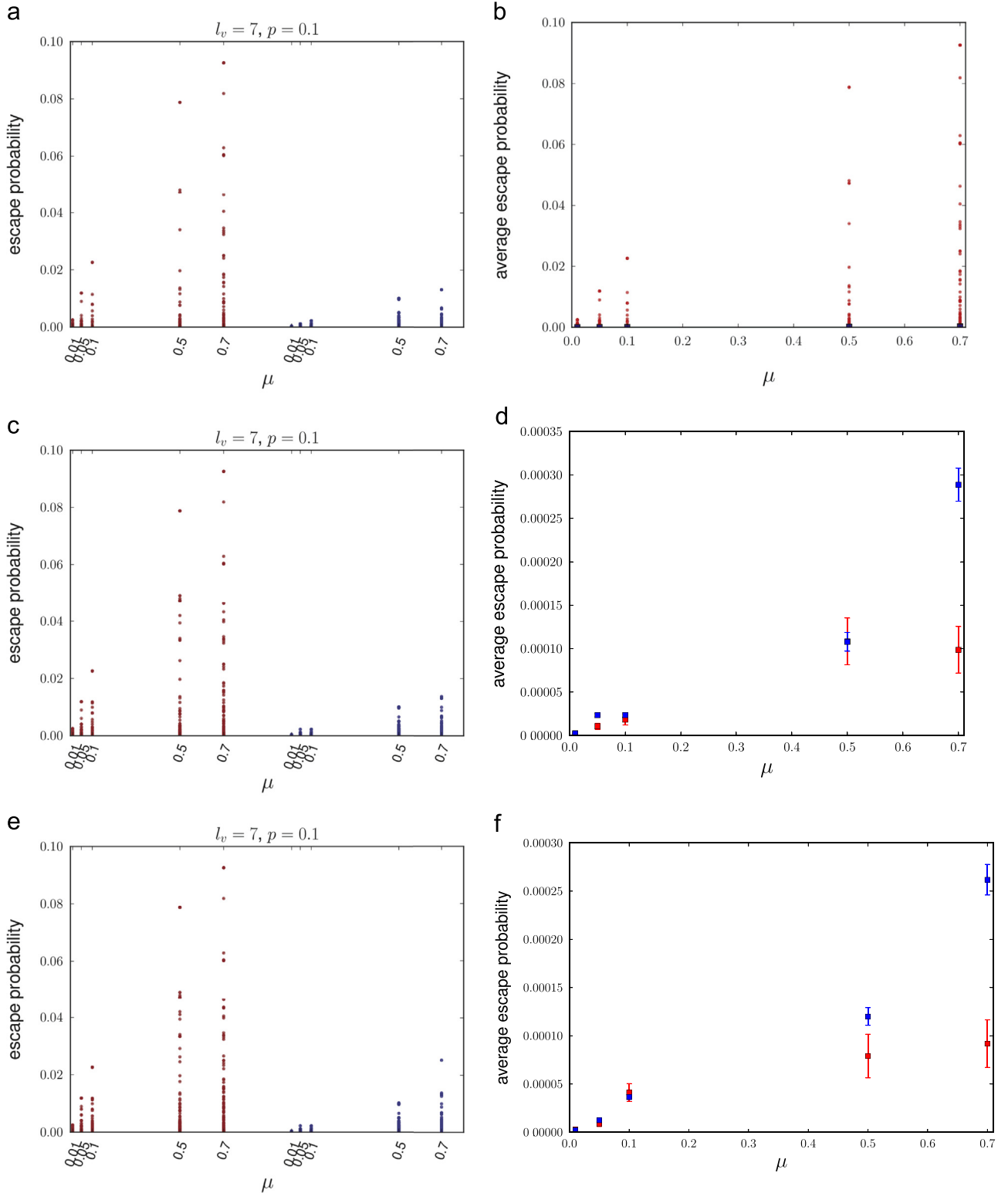


**Fig. 4.** Comparison between the long-term escape probability,  $P(N_E(\infty) > 0)$ , for  $B$  (red) and  $H$  (blue) genotype–phenotype graphs as the mutation rate,  $\mu$ , varies. Each row plot corresponds to a different graph from Fig. 2 (a)–(c),  $N_\nu = 1.5$ . For each graph, we fix an escape phenotype, and compute the escape probability for all remaining initial phenotypes. These plots show results for ten different escape phenotypes chosen at random. Plots (a), (c), and (e) show scatter plots for results for each initial condition, while plots (b), (d), and (f) show the escape probability averaged over initial conditions.  $\lambda = 0.1$  and  $\sigma = 0.9$ .

phenotypes are far less likely in genotype–phenotype maps associated to  $\nu N < 1$  (see Fig. 2(d) and (e)). Note that, although disjoint phenotype networks are much more likely for genotype–phenotype maps with  $\nu N > 1$ , it is possible to observe fully connected phenotype networks associated to  $\nu N > 1$ . An example is shown in

Fig. 2(a). Similarly, disjoint phenotype networks may also exist for  $\nu N < 1$ , although they are much less likely than the fully-connected ones. The emergence of disjoint subsets of phenotypes has an immediate consequence on evolutionary escape: since some phenotypes are unreachable, escape is not going to be

possible in the initial phenotype and the escape phenotype live in different disjoint subsets.

In order to gain a more quantitative understanding connectivity between phenotypes, we have plotted the distribution of the average distance between phenotypes corresponding to the data shown in Fig. 2. We have further computed the same data for the associated  $H$ -type genotype–phenotype graph: according to the procedure explained in Section 2, for each  $B$  genotype–phenotype map, we compute a  $H$  graph by randomly linking genotype–phenotype pairs under the constraint that both  $B$  and  $H$  graphs have the same phenotype degree distribution. Our results are shown in Fig. 3, from which a property stands out, namely,  $B$  genotype–phenotype graphs exhibit a much higher degree of heterogeneity than their  $H$ -type counterparts, as shown by the larger width of the distributions for  $B$ -type graphs (Fig. 3(a), (c), and (e)) compared to that of the distributions associated to  $H$ -graphs (Fig. 3(b), (d), and (f)).

### 3.2. The escape probability, $P(N_E(\infty) > 0)$ , exhibits higher degree of heterogeneity in $B$ graphs

Using the methods of Section 2.2, we have proceeded to compute the long-term escape probability  $P(N_E(\infty) > 0)$  for  $B$ -type genotype–phenotype graphs, i.e. those for which the nodes of the genotype network is the set of genotypes associated to viable phenotypes (see Section 2.1 and Supplementary materials), and compare to escape probability associated to  $H$ -type genotype–phenotype graphs, for which the genotype network is a hypercube.

Fig. 4 shows simulation results regarding how the escape probability,  $P(N_E(\infty) > 0)$ , changes as the mutation rate,  $\nu$ , is varied. Results are shown for both types of genotype–phenotype maps. We observe (see Fig. 4(a), (c), and (e)) that much higher levels of variability are obtained for  $B$ -type genotype–phenotype graphs. Such heterogeneity is directly inherited from the connectivity properties of  $B$  and  $H$  graphs (see Fig. 3): since the distance between phenotypes in  $H$  graphs is much more homogeneous than in  $B$  graphs so is the escape probability. Our analysis shows that the average escape probability (Fig. 4(b), (d), and (e)) is

not informative to distinguish between escape in either type of graph. Moreover, whereas this average is representative of the behaviour of  $H$  graphs, it is likely that for  $B$  graphs the average escape probability, due to their intrinsic heterogeneity, is not characteristic of their behaviour.

Furthermore, as a consequence of the heterogeneous behaviour of  $B$  genotype–phenotype graphs, one can find cases in which the escape probability on the  $B$  graph is an order of magnitude larger than on the  $H$  graph. In these instances, the theory of escape based on regular hypercube genotype spaces seriously under-estimates the escape probability.

### 3.3. Escape probability compared by distance between phenotypes

More conclusive results regarding the comparison between the behaviour of the escape probability on  $B$ - and  $H$ -class networks are obtained when we compare this quantity when considering that the distance between initial and escape phenotypes is the same on both types of networks. In other words, for each type of graph, we consider the change of the escape probability,  $P_E$ , as the distance between the initial and the escape phenotypes,  $n$ , varies. Given an initial phenotype and an escape phenotype, we define distance between them as the minimum path length between the neutral networks of both phenotypes, i.e. we compute the path length between all the pairs of genotypes belonging to these neutral networks and take the minimum of these distances as the distance between phenotypes. We then compare the escape probability for couples of initial and escape phenotypes in both  $B$  and  $H$  networks at the same distance.

Our results are shown in Fig. 5. We observe that, just as with our results of the previous section,  $B$ -class networks exhibit a larger degree of heterogeneity than their  $H$ -class counterparts. This is most clearly reflected in the fact that  $B$ -class networks exhibit a much wider range of distances between phenotypes. However, within the range of phenotype distances shared by both types of networks, we observe that for smaller phenotype distances, the topological structure of  $B$ -class networks facilitates escape as the escape probabilities are larger for this type of graph.

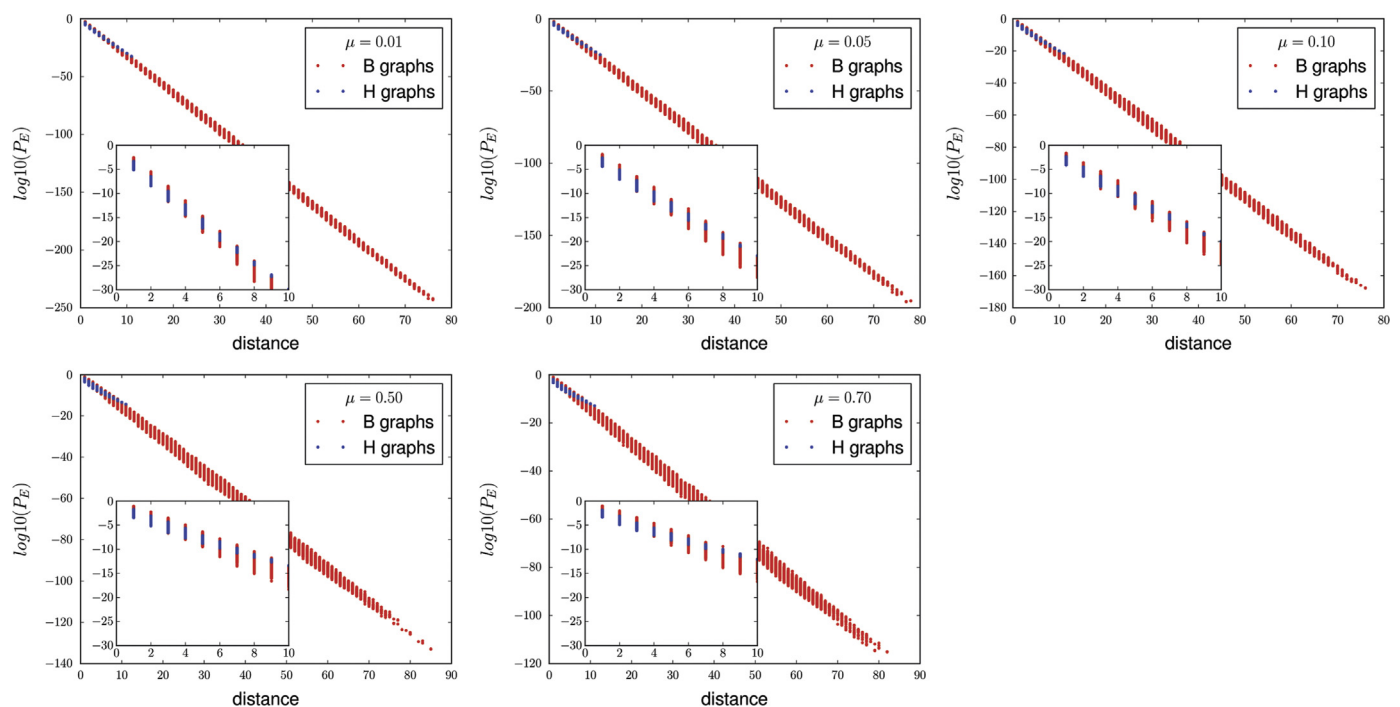
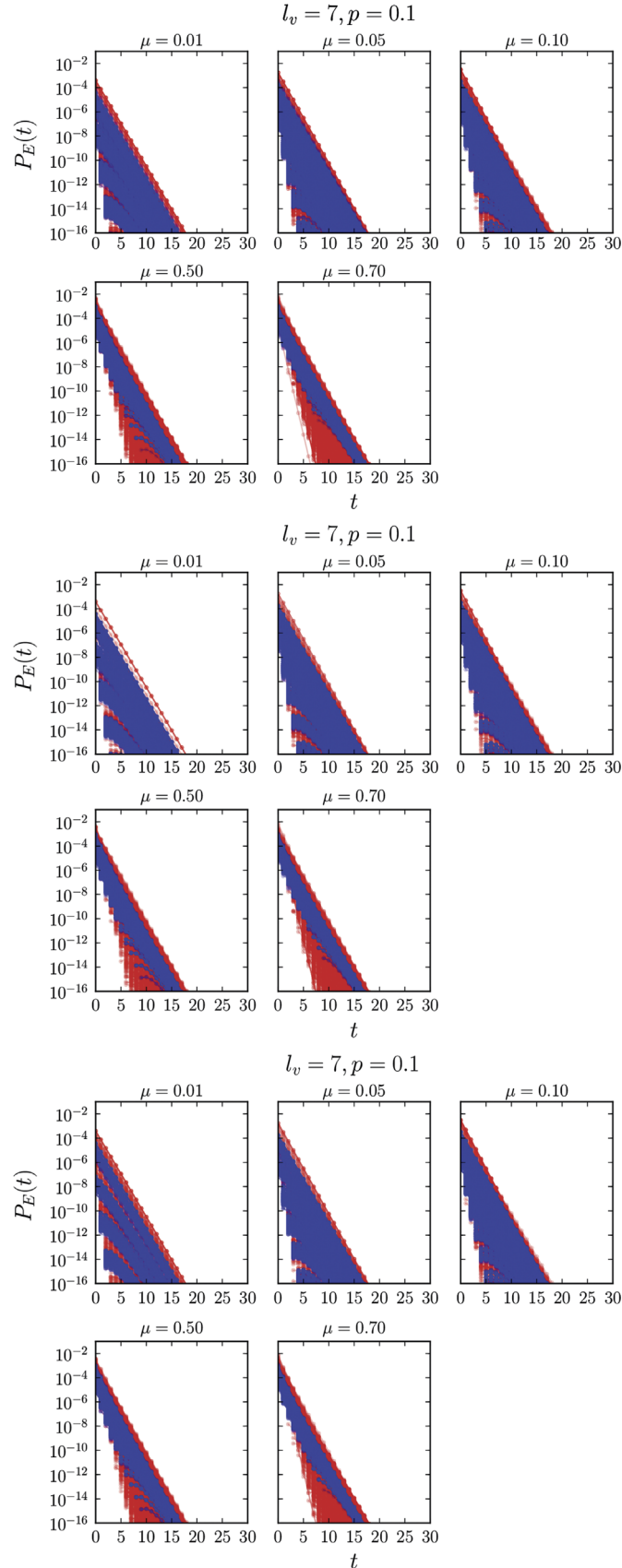


**Fig. 5.** Series of plots comparing probability of escape in a log scale, at large time, on  $B$  (red) and  $H$  (blue) genotype–phenotype graphs by same distance between phenotypes. Each plot corresponds to a different mutation rate  $\nu$  (up to bottom and left to right:  $\nu = 0.01, 0.05, 0.1, 0.5, 0.7$ ). Escape on  $H$  graphs has not been observed for greater distances. (For interpretation of the references to colour in this figure caption, the reader is referred to the web version of this paper.)

However as, we consider escape between more distant phenotypes, the situation reverses as the regular structure of  $H$ -type graphs appears to promote escape.



### 3.4. Escape dynamics: asymptotic behaviour of $P_E(t)$

We now proceed to compare the behaviour of the escape probability at time  $t$ ,  $P_E(t)$  for graphs of both  $B$  and  $H$  classes. Our results are shown in Fig. 6. From these results we conclude that  $P_E(t)$  decay exponentially for large  $t$ . Also we observe that a larger degree of variability is observed for  $B$ -type genotype-phenotype graph. This fact is a direct consequence of the richer structure which characterises  $B$ -class graphs.

In order to analyse the asymptotic behaviour of  $P_E(t)$ , Eq. (9), we consider the change of variable  $\vec{\theta}_t = \vec{\theta}_\infty + \vec{e}_t$  in the recursion relation Eq. (9):

$$\begin{aligned} \vec{\theta}_\infty + \vec{e}_{t+1} &= \sigma \cdot \vec{1} + \lambda(B \cdot (\vec{\theta}_\infty + \vec{e}_t)) \odot (B \cdot (\vec{\theta}_\infty + \vec{e}_t)) \\ &= \sigma \cdot \vec{1} + \lambda \left( B \cdot \vec{\theta}_\infty \odot B \cdot \vec{\theta}_\infty + 2B \cdot \vec{e}_t \odot B \cdot \vec{\theta}_\infty + B \cdot \vec{e}_t \odot B \cdot \vec{e}_t \right). \end{aligned} \quad (15)$$

where  $\vec{\theta}_\infty$  satisfies (12), which implies that  $\vec{e}_t$  satisfies the following recursion relation:

$$\vec{e}_{t+1} = \lambda(2B \cdot \vec{e}_t \odot B \cdot \vec{\theta}_\infty + B \cdot \vec{e}_t \odot B \cdot \vec{e}_t) \quad (16)$$

Moreover, asymptotically, when  $t \rightarrow \infty$ ,  $(\vec{e}_t)_i \ll 1$ , so that one can linearise Eq. (16):

$$\vec{e}_{t+1} = \lambda(2B \cdot \vec{e}_t \odot B \cdot \vec{\theta}_\infty). \quad (17)$$

Recalling that  $B = \nu D^{-1}A + (1 - \nu)Id$ , ff  $\nu \ll 1$  then  $B = Id$  and, consequently,  $\vec{\theta}_\infty = \vec{\theta}_0$ . This implies that the asymptotic behaviour of  $(\epsilon_t)_i$  is determined by the recursion relation  $(\epsilon_{t+1})_i = 2\lambda(\epsilon_t)_i$ , i.e.

$$(\epsilon_t)_i \approx (2\lambda)^t \quad (18)$$

Eq. (18) allows us to determine the asymptotic behaviour of  $P_E(t)$  for  $\nu \ll 1$ . Since  $P_E(t) = (\vec{\theta}_{t-1} - \vec{\theta}_t)_i = (\vec{e}_{t-1} - \vec{e}_t)_i \approx (2\lambda)^t ((2\lambda)^{-1} - 1)$ . This result shows that, for negligible small values of the mutation rate, the escape probability decays exponentially as  $P_E(t) \approx e^{\log(2\lambda)t}$  with  $2\lambda < 1$ , independently of network topology.

Fig. 6 shows simulation results for different  $B$  and  $H$  genotype-phenotype networks and for different values of the mutation rate,  $\nu$ . These numerical results show that, even for non-negligible values of the mutation rate  $\nu$ , the asymptotic behaviour of  $P_E(t)$  is exponential, i.e.  $P_E(t) \approx e^{-st}$  for large  $t$ , although the rate associated to the exponential distribution is indeed dependent on the mutation rate, so that, in general,  $s \neq -\log(2\lambda)$  ( $2\lambda < 1$ ).

We further observe a great deal of heterogeneity in the behaviour of  $P_E(t)$  associated to  $B$  genotype-phenotype networks (see Figs. 6 and 7). Fig. 7 shows how the histograms of the distribution of rates  $s$  change as the parameter values used to generate  $B$ -type genotype-phenotype graphs (see Supplementary Materials and Ibáñez-Marcelo and Alarcón, 2014 for details) are varied. These results show that, regardless of the parameter values, the dispersion observed in the rate  $s$  associated to  $B$  networks is robustly larger than for their  $H$ -counterparts.

Further information regarding the difference between evolutionary escape on  $B$  and  $H$  genotype-phenotype graphs can be obtained by recalling that, as the escape time is exponentially distributed,  $P_E(t) \approx e^{-t/\tau_E}$ , where  $\tau_E$  is the average escape time. The distributions of  $s$  associated to  $B$ - and  $H$ -type graphs, Fig. 7, show

**Fig. 6.** Series of plots showing the escape probability at time exactly  $t$ ,  $P_E(t)$  for different genotype-phenotype maps (correspond to graphs in Fig. 2 (a)–(c),  $N_\nu = 1.5$ ) with different values of the mutation rate,  $\nu$ . Red corresponds to  $B$  graphs and blue to  $H$  graphs (blue dots overlay red dots). For each  $B$  graph, we have set an escape phenotype and calculate the probability of escape for all possible initial conditions. We have repeated this computation for ten randomly chosen escape phenotypes for each graph. Parameters:  $\lambda = 0.1$ ,  $\sigma = 0.9$ . Note that the theory developed in Section 3.4 is not applicable here as  $\nu = 0.7$ . (For interpretation of the references to colour in this figure caption, the reader is referred to the web version of this paper.)

that the values of  $s$  corresponding to escape on  $B$  genotype–phenotype graphs are shifted to the left with respect to their counterparts on  $H$ -graphs, which implies that the average escape time on  $B$ -type graphs is bigger than that on  $H$ -type graphs.

### 3.5. Escape dynamics: escape time probability conditioned to escape

We now proceed to analyse the escape time probability conditioned to eventual escape,  $P_E(t|E) = P(N_E(t) > 0 \wedge N_E(t-1) = 0 | N_E(\infty) > 0, N_i(0) = 1, N_j(0) = 0 \quad \forall j \neq i)$ . The rationale for looking at the properties of this particular function follows from our results regarding the connectivity structure of  $B$ -type graphs in which we have seen that phenotypes may be disconnected, and therefore the probability of reaching certain escape phenotypes within  $B$ -type graphs may be zero. By conditioning to eventual escape, we discard these cases and focus on the escape process within connected phenotype components.

Comparative analysis between the behaviour of the conditioned escape time probability,  $P_E(t|E)$ , on  $B$ - and  $H$ -type graphs shows that there are striking quantitative differences between them. Whereas  $P_E(t|E)$  on  $H$ -type graphs is sharply concentrated around a well-defined average escape time,  $P_E(t|E)$  on  $B$ -type graphs is virtually flat, very close to a uniform distribution, where the average escape time has barely any representative.

This behaviour is a direct consequence of the distribution of average distances between phenotypes shown in Fig. 3 associated to both types of genotype–phenotype graph: while  $H$ -graphs exhibit distributions of average distances between phenotypes which are sharply concentrated around the average value, distance distributions for  $B$ -graphs are much wider with an average value that is rather unrepresentative of the behaviour of the ensemble

of realisations of the escape process. These properties have a direct effect on the escape time subject to eventual escape.

### 3.6. Escape on $H$ -graphs with mutations and viability conditions

In this section, we consider a different setting regarding our population dynamics. Rather than introducing viability conditions at the level of the topology of the genotype–phenotype network (i.e. running the escape process on a  $B$ -class network generated according to the model described in the Supplementary Materials), we consider the escape dynamics on a  $H$ -type network (i.e. the full genotype space) and introduce the viability conditions at the population dynamics level: if a mutation of a viable individual leads to a non-viable genotype (see Supplementary Materials for the definition of our viability conditions), the mutated descendants are killed. We denote this new scenario as the  $H_{vc}$ -class. The simulation results corresponding to this scenario are shown in Figs. 9 and 10, where we show how the escape probability changes as the mutation rate,  $\nu$ , and the distance between the initial and escape phenotypes,  $n$ , vary, respectively. Contrary to our previous results, the  $H$ -class scenario favours escape when compared to the  $H_{vc}$  scenario, as the escape probabilities for the latter are systematically smaller than for the former. This is due to the fact that the viability conditions effectively renormalise the death rate of the  $H_{vc}$ : non-viable mutations elevate the death rate with respect to the  $H$ -class scenario.

## 4. Discussion and conclusions

In this paper we have studied the problem of evolutionary escape from a novel perspective, namely, since selective pressures

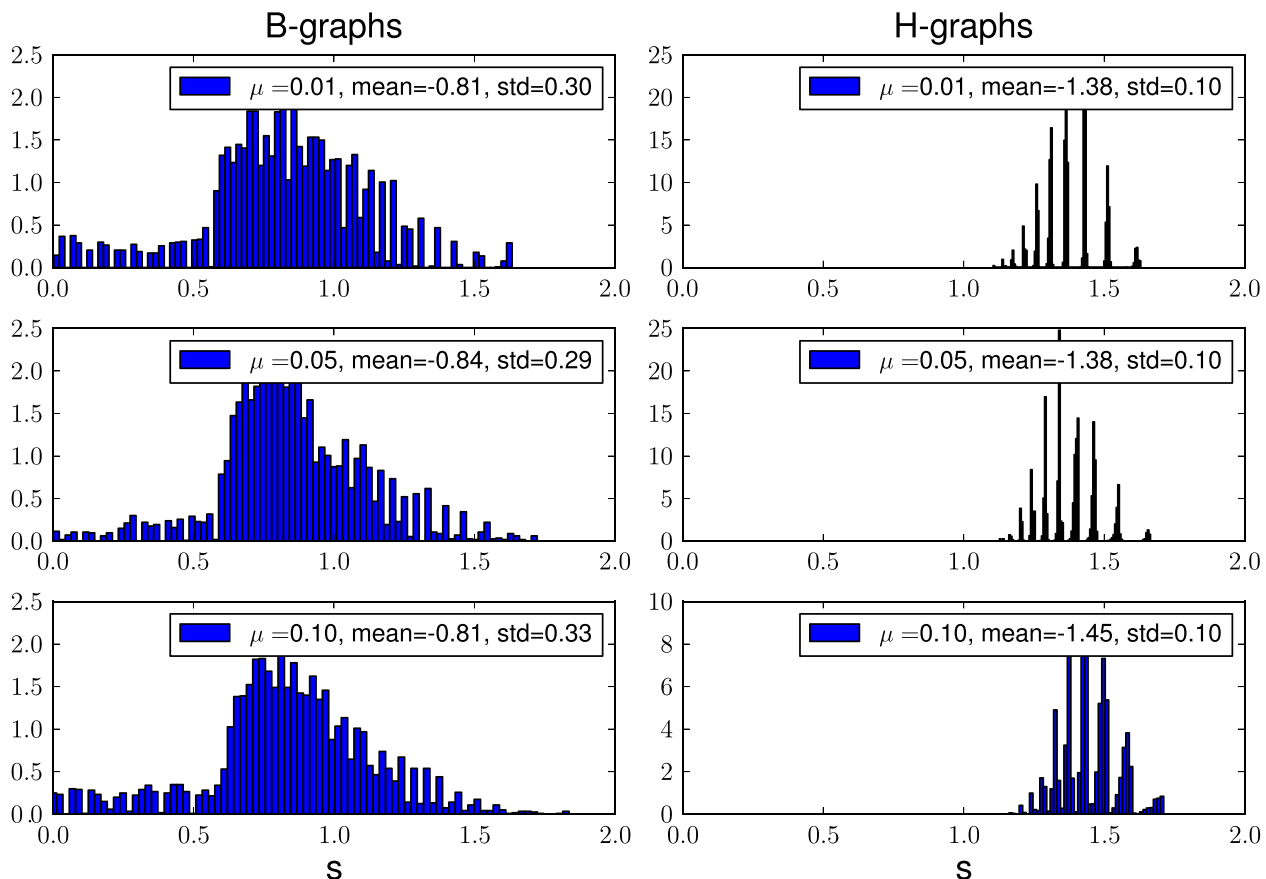
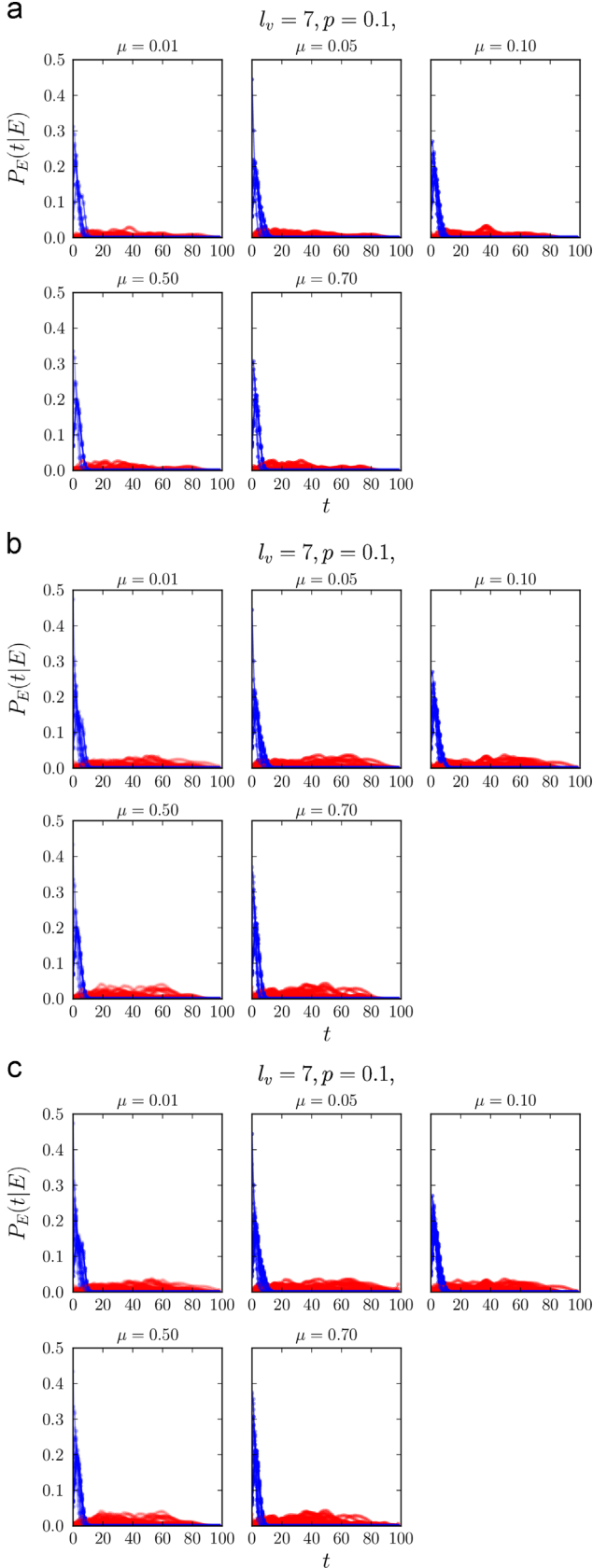


**Fig. 7.** Series of plots showing the rate,  $s$ , associated to  $P_E(t) \sim e^{-st}$ , for different genotype–phenotype graphs of type  $B$  (left column, graphs correspond to Fig. 2 (a)–(c) with  $N_\nu = 15$ ) and type  $H$  (right column). The value of  $s$  for each graph is obtained by fitting the data shown in Fig. 6.

act on phenotypes rather than genotypes and therefore fitness is determined by the former, escape problems should be analysed within the context of complex genotype–phenotype networks rather than on regular, hypercube genotype lattices where fitness is directly determined by the genotype.



We have carried out a comparative analysis considering two types of genotype–phenotype networks. We have considered complex genotype–phenotype networks, our so-called *B*-type graphs, which are generated according to a multi-scale model proposed in Ibáñez-Marcelo and Alarcón (2014) (and summarised in the Supplementary Materials). Associated to each *B*-graph, we generate a *H*-type genotype–phenotype graph, which, according to the procedure explained in Section 2, is computed by randomly linking genotype–phenotype pairs under the constraint that both *B* and *H* graphs have the same phenotype degree distribution (see Supplementary Materials). We have further formulated a population dynamics model, consisting of a multi-type branching process (Kimmel and Axelrod, 2002), where types are associated to genotypes and their proliferation probability is assigned according to the corresponding phenotype, as determined by the either *B* or *H* genotype–phenotype map.

Our comparative analysis sheds some light on the differences between the escape process on either type of genotype–phenotype network, regarding both dynamical and steady-state properties. We have started our analysis by studying the average distance between phenotypes, as this property directly affects the escape process (see Section 3.1). Our results (Fig. 3) show that, whereas the distribution of distance between phenotypes in *H*-type genotype–phenotype graphs is sharply peaked around its mean value, its counterpart for *B*-graphs exhibits a much larger degree of dispersion so that the average distance is hardly representative of individual behaviour within the statistical ensemble.

An alternative to the approach used in Section 3.1, which is based on computing the average shortest path between phenotypes, consists of resorting to spectral graph theory (Chung, 1992). In fact, Chung (1989) has proven that the diameter of a graph, i.e. the maximum of the distances among all possible pairs of vertices, is small (i.e.  $O(\log n)$  where  $n$  is the number of nodes) if the modulus of the second eigenvalue of the adjacency matrix is small compared to the first eigenvalue. However, in our case, this method does not allow us to discriminate between *B* and *H* graphs, nor to identify heterogeneities among *B*-graphs, as per the examples shown in Fig. 2. This is a direct consequence of the fact that genotype subgraph for both *B* and *H* genotype–phenotype maps are bipartite graphs.

Consider an *H* graph whose genotype subgraph,  $G_H$ , is an  $n$ -cube, i.e. a  $2^n$ -vertices hypercube where one can assign to each vertex a string of length  $n$  from  $(-1, -1, \dots, -1)$  to  $(1, 1, \dots, 1)$ . For example, a 2-cube (or square) would be

00, 01, 10, 11.

One can now define two disjoint subsets within the graph  $G = (X, Y)$ . Where  $X = \{\text{vertices who have an even number of 1's}\}$  and  $Y = \{\text{vertices who have an odd number of 1's}\}$ . Since edges connect nodes that differ by one entry in the label string, we only have edges between  $X$  and  $Y$ , thus constructing a colouring with only two colours and, therefore, the  $n$ -cube graph is bipartite. Since the genotype subgraph of a *B* genotype–phenotype network is a subset of  $G_H$  (see reference Ibáñez-Marcelo and Alarcón, 2014 and the Supplementary Materials), then it also is a bipartite graph. Bipartite graphs happen to have rather trivial spectral properties (Brower and Haemers, 2012): bipartite networks have symmetric spectra and the spectral gap is equal to zero. *B* and *H* networks are not exactly bipartite, because of the presence of the phenotype nodes. However, we have checked that these nodes perturb the spectrum only very slightly. Therefore, the spectral properties

**Fig. 8.** Series of plots comparing the behaviour of the conditioned escape time probability,  $P_E(t|E)$ , on *B*- (red lines) and *H*-type (blue lines) genotype–phenotype maps. The *B*-graphs considered in plots (a), (b) and (c) are the same as those whose connectivity is shown in Fig. 2(a), (b), and (c), respectively and  $N_\nu = 15$ . By studying how  $P_E(t|E)$  changes as the mutation rate,  $\mu$ , varies, we observe that  $P_E(t|E)$  is rather robust to changes in this parameter. (For interpretation of the references to colour in this figure caption, the reader is referred to the web version of this paper.)



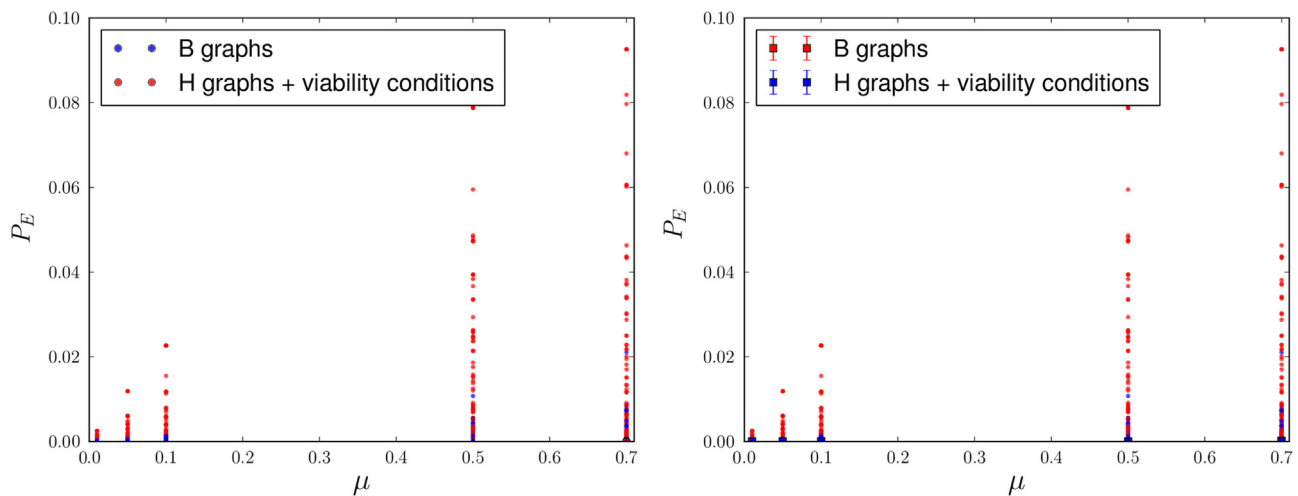


**Fig. 9.** Comparison between the long-term escape probability,  $P(N_E(\infty) > 0)$ , for  $H+$  viability conditions (red) and  $H$  (blue) genotype-phenotype graphs as the mutation rate,  $\mu$ , varies. Left: All samples. Right: Mean confidence intervals at 95%. (For interpretation of the references to colour in this figure caption, the reader is referred to the web version of this paper.)

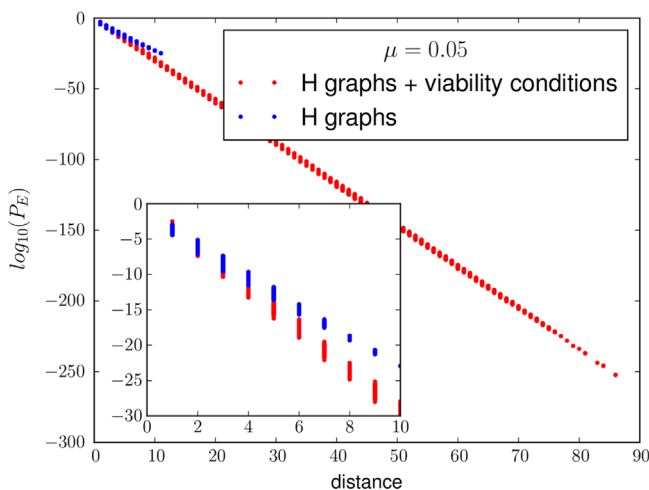


**Fig. 10.** Comparison between the long-term escape probability,  $P(N_E(\infty) > 0)$ , for  $H+$  viability conditions (red) and  $H$  (blue) genotype-phenotype graphs by distance between phenotypes. Mutation rate:  $\mu = 0.05$ . (For interpretation of the references to colour in this figure caption, the reader is referred to the web version of this paper.)

associated to these two types of networks are not the right framework to analyse the differences between them, in particular, those concerning the evolutionary escape problem.

The heterogeneity observed in the distribution of distances between phenotypes in  $B$ -type graphs induces heterogeneous behaviour in all the observables associated to the escape problem that we have investigated. The escape probability in  $B$ -type graphs displays a much wider range of variability than in  $H$ -type networks, with instances in which the escape probability in the  $B$ -graph is an order of magnitude bigger than in its  $H$ -type counterpart (see Fig. 4). The comparison between the escape probability on  $H$ - and  $B$ -type networks is much clarified when analysed in terms of the distance between the initial and the escape phenotypes: when we consider the escape probability for fixed distance between phenotypes, we observe that for close phenotypes the topology of  $B$ -class networks facilitates escape. As the distance between the initial and the escape phenotypes increases, escape is more likely to occur in  $H$ -class networks (see Fig. 5).

Heterogeneity is also ubiquitous when dynamical properties are examined. Fig. 7 shows that the average escape time is much more homogeneously distributed in  $H$ -type graphs. Furthermore,

as a result of the heterogeneity in the average escape time for  $B$ -graphs, we have determined that escape is very likely to occur on considerable longer time scales on  $B$ -graphs. When studying the escape time distribution conditioned to eventual escape (see Fig. 8), we observe that, unlike  $H$ -graphs where escape exhibits a well-defined, characteristic time scale, conditioned escape time on  $B$ -graphs shows a much wider (almost uniform) distribution with virtually no discernible characteristic scale.

Therefore, unlike genotype-phenotype graphs where the genotype network is a regular hypercubic lattice, where averaged properties are representative of individual behaviour within the statistical ensemble, in complex genotype-phenotype networks heterogeneity is the rule. This implies that predictions regarding emergence of resistant varieties in, for example, cancer cell populations under treatment (Tian et al., 2011) based on regular hypercubic genotype spaces may be inaccurate. Rather, a more detailed study of the underlying genotype-phenotype structure is necessary to produce accurate estimates. The application of our methods to the issue of emergence of resistance in tumours under therapy would require to develop a model of the gene regulatory network governing the appearance of pathological cell states (i.e. malignant phenotype) as well as the corresponding epigenetic regulation (Roesch et al., 2010), and then analyse the corresponding genotype-phenotype graph to discern how deregulations at the genetic and epigenetic levels would affect evolutionary escape, whereby targeted strategies aimed at minimising the escape probability could be formulated. The formulation of such models is beyond the scope of this work and left for future research.

## Acknowledgements

The authors gratefully acknowledge the Spanish Ministry for Science and Innovation (MICINN) for funding under grant MTM2011-29342 and Generalitat de Catalunya for funding under grant 2014SGR1307.

## Appendix A. Supplementary data

Supplementary data associated with this paper can be found in the online version at <http://dx.doi.org/10.1016/j.jtbi.2015.12.033>.

## References

- Aguirre, J., Buldú, J.M., Stich, M., Manrubia, S.C., 2011. Topological structure of the space of phenotypes: the case of RNA neutral networks. *PLoS One* 6, e26324.
- Alarcon, T., Jensen, H.J., 2010. Quiescence: a mechanism for escaping the effects of drug on cell populations. *J. R. Soc. Interface* 8, 99–106.
- Alarcon, T., Byrne, H.M., Maini, P.K., 2005. A multiple scale model of tumour growth. *Multiscale Model. Simul.* 3, 440–475.
- Balaban, N.Q., Merrin, J., Chait, R., Kowalik, L., Leibler, S., 2004. Bacterial persistence as a phenotypic switch. *Science* 305, 1622–1625.
- Bergman, A., Siegal, M.L., 2003. Evolutionary capacitance is a general feature of complex gene networks. *Nature* 424, 549–552.
- Brikci, F.B., Clairanbault, J., Ribba, B., Perthame, B., 2008. An age-and-cyclin-structured cell population model for healthy and tumoural tissues. *J. Math. Biol.* 57, 91–110.
- Bristow, R.C., Hill, R.P., 2008. Hypoxia, DNA repair and genetic instability. *Nat. Rev. Cancer* 8, 180–192.
- Brower, A.R., Haemers, W.H., 2012. *Spectra of Graphs*. Springer, New York, NY, USA.
- Chung, F.R.K., 1989. Diameter and eigenvalues. *J. Am. Math. Soc.* 2, 187–196.
- Chung, F.R.K., 1992. *Spectral Graph Theory*. American Mathematical Society, USA.
- Ciliberti, S., Martin, O.C., Wagner, A., 2007. Robustness can evolve gradually in complex regulatory gene networks with varying topology. *PLoS Comput. Biol.* 3 (2), e15.
- Ciliberti, S., Martin, O.C., Wagner, A., 2007. Innovation and robustness in complex regulatory gene networks. *Proc. Natl. Acad. Sci.* 104, 13591–13596.
- Delvenne, J.C., Yaliraki, S.N., Barahona, M., 2010. Stability of graph communities across time scales. *Proc. Natl. Acad. Sci.* 107, 12755–12760.
- Fontana, W., Schuster, P., 1998. Shaping space: the possible and the attainable in RNA genotype–phenotype mapping. *J. Theor. Biol.* 194, 491–515.
- Ibáñez-Marcelo, E., Alarcon, T., 2014. The topology of robustness and evolvability in evolutionary systems with genotype–phenotype map. *J. Theor. Biol.* 356, 144–162.
- Iwasa, Y., Michor, F., Nowak, M.A., 2003. Evolutionary dynamics of escape from biomedical intervention. *Proc. R. Soc. Lond. B* 270, 2573–2578.
- Iwasa, Y., Michor, F., Nowak, M.A., 2004. Evolutionary dynamics of invasion and escape. *J. Theor. Biol.* 226, 205–214.
- Jaeger, J., Monk, N., 2014. Bioattractors: dynamical systems theory and the evolution of regulatory processes. *J. Physiol.* 592, 2267–2281.
- Kauffman, S.A., 1993. *The Origins of Order*. Oxford University Press, New York, U.S.A.
- Kimmel, M., Axelrod, D.E., 2002. *Branching Processes in Biology*. Springer-Verlag, New York, NY, USA.
- Lambiotte, R., Delvenne, J.C., Barahona, M., 2009. Laplacian dynamics and multi-scale modular structure in networks, [arxiv:0812.1770](https://arxiv.org/abs/0812.1770).
- Lewis, K., 2007. Persister cells, dormancy and infectious disease. *Nat. Rev. Microbiol.* 5, 48–56.
- Lipman, D., Wilbur, W., 1991. Modelling neutral and selective evolution of protein folding. *Proc. R. Soc. Lond. B* 245, 1–7.
- Ndifon, W., Plotkin, J.B., Dushoff, J., 2009. On the accessibility of adaptive phenotypes of a bacterial metabolic network. *PLoS Comput. Biol.* 5, e1000472.
- Rodrigues, J.F., Wagner, A., 2009. Evolutionary plasticity and innovations in complex metabolic reaction networks. *PLoS Comput. Biol.* 5, e1000613.
- Rodrigues, J.F., Wagner, A., 2011. Genotype networks in sulfur metabolism. *BMC Syst. Biol.* 5, 39.
- Roesch, A., Fukunaga-Kalabis, M., Schmidt, E.C., Zabierowski, S.E., Brafford, P.A., Vultur, A., Basu, D., Gimotty, P., Vogt, T., Herlyn, M., 2010. A temporarily distinct subpopulation of slow-cycling melanoma cells is required for continuous tumor growth. *Cell* 141, 583–594.
- Sagitov, S., Serra, M.C., 2009. Multitype Bienayme–Galton–Watson processes escaping extinction. *Adv. Appl. Probab.* 41, 225–246.
- Samal, A., Rodrigues, J.F., Jost, J., Martin, O.C., Wagner, A., 2010. Genotype networks in metabolic reaction spaces. *BMC Syst. Biol.* 4, 30.
- Schaub, M.T., Delvenne, J.C., Yaliraki, S.N., Barahona, M., 2010. Markov dynamics as a zooming lens for multiscale community detection: non clique-like communities and the field-of-view limit. *PLoS One* 7, e32210.
- Schuster, P., Fontana, W., Stadler, P., Hofacker, I.L., 1994. From sequences to shapes and back: a case study in RNA secondary structures. *Proc. R. Soc. Lond. B* 255, 279–284.
- Serra, M.C., Haccou, P., 2007. Dynamics of escape mutants. *Theor. Popul. Biol.* 72, 167–178.
- Serra, M.C., 2006. On the waiting time to escape. *J. Appl. Probab.* 43, 296–302.
- Siegal, M.L., Bergman, A., 2002. Waddington's canalization revisited: developmental stability and evolution. *Proc. Natl. Acad. Sci.* 99, 10528–10532.
- Tian, T., Olson, S., Whitacre, J.M., Harding, A., 2011. The origin of cancer robustness and evolvability. *Integr. Biol.* 3, 17–30.
- Wagner, A., 1996. Does evolutionary plasticity evolve? *Evolution* 50, 1008–1023.
- Wagner, A., 2007. *Robustness and Evolvability in Living Systems*. Princeton University Press, Princeton, NJ, U.S.A.
- Wagner, A., 2008. Neutralism and selectionism: a network-based reconciliation. *Nat. Rev. Genet.* 9, 965–974.
- Wagner, A., 2008. Robustness and evolvability: a paradox resolved. *Proc. R. Soc. B* 275, 91–100.
- Wagner, A., 2011. Genotype networks shed light on evolutionary constraints. *Trends Ecol. Evol.* 26, 577–583.
- Wagner, A., 2012. The role of robustness in phenotypic adaptation and innovation. *Proc. R. Soc. B* 279, 1249–1258.